



Kinetic model for sonolytic degradation of non-volatile surfactants: Perfluoroalkyl substances



Takshak Shende, Gangadhar Andaluri, Rominder P.S. Suri*

NSF – Water and Environmental Technology (WET) Center, Civil and Environmental Engineering Department, Temple University, Philadelphia, PA 19122, USA

ARTICLE INFO

Keywords:
Sonochemical catalysis
Perfluoroalkyl substances
PFAS
PFOA
PFOS
Ultrasound

ABSTRACT

Sonolytic degradation kinetics of non-volatile surfactant perfluorooctanoic acid (PFOA) and perfluorooctane sulfonic acid (PFOS) were investigated over a range of concentration, considering active cavity as a catalyst. The Michaelis-Menten type kinetic model was developed to empirically estimate the concentration of active cavity sites during reactions. Sonolytic degradation of PFOA and PFOS, as well as the formation of its inorganic constituents, fluoride, and sulfate, follows saturation kinetics of pseudo-first order at lower concentration ($< 2.34 \mu\text{M}$) and zero order at higher concentration ($> 23.60 \mu\text{M}$). Nitrate and hydrogen peroxide formations were $0.53 \pm 0.14 \mu\text{M}/\text{min}$ and $0.95 \pm 0.11 \mu\text{M}/\text{min}$, respectively. At a power density of 77 W/L and frequency of 575 kHz, the empirically estimated maximum number of active cavity sites that could lead to the sonolytic reaction were 89.25 and 8.8 mM for PFOA and PFOS, respectively. This study suggests that a lower number of active cavity sites with higher temperature needed to degrade PFOS might be the reason for lower degradation rate of PFOS compared to that of PFOA. Diffusion of non-volatile surfactants at the cavity-water interface is found to be the rate-limiting step for the mineralization of perfluoroalkyl substances.

1. Introduction

Poly-and perfluoroalkyl substances (PFAS) are a subset of aliphatic compounds of which fluorine atoms replace one or more hydrogen atom [1]. Chemical stability, thermal inertness, lipophobic and hydrophobic nature, and ability to lower surface tension in an aqueous solution allowed PFASs utilization in the eclectic industrial process and consumer application [1]. Perfluorooctanoic acid (PFOA) and perfluorooctane sulfonic acid (PFOS) surfactants are contaminants of emerging concern (CECs) due to their persistent nature, widespread distribution in the environmental matrix, and potential of being carcinogenic [2,3]. In 2016, the United States Environmental Protection Agency (US EPA) has established a drinking water health advisory for the combined concentration of PFOA and PFOS at 70 ppt. Hence, PFOA and PFOS were selected as model PFAS compounds for this study. A number of studies have examined the degradation of PFAS using electrochemical oxidation [4,5], photo-catalysis [6], and activated persulfate [7] amongst other [8]. Campbell and Hoffman (2015) observed insignificant degradation of PFAS at an ultrasonic frequency of 20 kHz using probe sonication [9]. Many studies reported high-frequency ultrasound ($> 202 \text{ kHz}$), which uses a vibrating flat plate transducer, as a promising technology to mineralize PFOA and PFOS [10–12]. However, the sonochemical process optimization would benefit from a deeper

understanding of the dynamics of PFAS adsorption at the collapsible cavity-water interface.

Soundwaves, with a frequency higher than 18 kHz, have been extensively studied for the degradation of many organic contaminants [13–16]. Compression and rarefaction phases of the sound wave produce cavitation in the aqueous solution that adiabatically collapses to create a microenvironment with high temperature (4000–10,000 K) and pressure (1000 bar) [17–19]. It is considered that heat produced at these microscopic points thermally breaks down chemicals in the vicinity. Thermal breakdown of the water vapors in the cavity generates highly reactive radicals which subsequently enter into the bulk water to oxidize chemicals [13,20]. The reaction rate of the sonolytic system can be considered as a function of the number of active cavities produced in the solution and rectified diffusion of the contaminants and water into the cavity.

High Henry's constant and vapor pressure allows diffusion of the volatile organic compound into the cavity. However, diffusion of non-volatile compounds is lower due to low Henry's constant and resistance to rectified diffusion at the cavity-water interface. Adsorption of non-volatile compounds, such as a surfactant, at the cavity-water interface, can lead to their degradation [21–24]. Equilibrium partitioning based Langmuir-Hinshelwood type kinetic model has been widely studied to model adsorption-dependent degradation of the surfactants [21–24].

* Corresponding author.

E-mail addresses: takshak@temple.edu (T. Shende), gangadhar@temple.edu (G. Andaluri), rsuri@temple.edu (R.P.S. Suri).

<https://doi.org/10.1016/j.ultsonch.2018.08.028>

Received 17 July 2018; Received in revised form 14 August 2018; Accepted 27 August 2018

Available online 05 September 2018

1350-4177/ © 2018 Elsevier B.V. All rights reserved.

Vecitis et al. (2008) [25] ascertained that highly recalcitrant non-volatile surfactants such as perfluoroalkyl substances (PFAS), thermally break down at the hydrophilic (sulfonate or carboxylate) part of molecule at the cavity-water interface to form a volatile fluorinated intermediate, which subsequently enters the cavity to get thermally mineralized into its inorganic components such as fluoride, sulfate, carbon monoxide, carbon dioxide, and volatile PFAS compounds [25]. However, an equilibrium partitioning approach adopted by Vecitis et al. (2008) to model degradation kinetics of PFAS could not explain PFAS adsorption dynamics at the cavity-water interface [25]. Though theoretical consideration of Langmuir-Hinshelwood mechanism (surface catalysis), and Michaelis-Menten mechanism (enzyme catalysis) are distinct, both models are based on heterogeneous catalysis. Besides, saturation-based kinetics involved in both models is typically driven by the affinity of contaminants with the catalyst. Thus, sonolytic degradation kinetics of non-volatile surfactants could also be modeled using Michaelis-Menten mechanism, considering an active cavity as a catalyst, similar to enzymes.

Michaelis-Menten kinetic model has been used to model degradation of organic compounds in the presence of catalysts and ultrasound [26,27]. However, ultrasonic degradation kinetics considering active cavity as a catalyst is not examined. Ultrasonic decomposition of surfactants is a function of adsorption of surfactants at the cavity-water interface. Thus, Michaelis-Menten theory could be utilized to estimate the number of active cavity sites participating in the reactions empirically and to understand the nature of the cavity-water interface of the collapsible cavity. Perfluorooctanoic acid (PFOA) and perfluorooctane sulfonic acid (PFOS) would be model compounds because they are resistant to degraded by hydroxyl radicals [8] but can undergo thermal degradation at elevated temperature [28]. This study examines the Michaelis-Menten type kinetics to model degradation kinetics of a mixture of non-volatile surfactants, PFOA and PFOS, and discusses an empirical number of active cavity sites participating in sonolytic reactions.

2. Materials and methods

2.1. Chemicals and reagents

Analytical grade perfluorooctanoic acid (PFOA, 96%); perfluorooctane sulfonic acid potassium salt (PFOS, 98%) were purchased from Sigma-Aldrich, USA. Stable-isotope surrogates $^{13}\text{C}_8$ PFOA (99%) and $^{13}\text{C}_8$ PFOS (99%) were purchased from Cambridge Isotope Laboratories, Inc. HPLC grade methanol (> 99.8%), acetonitrile (> 99.9%), and HPLC grade water were purchased from Sigma-Aldrich. Concentrated sulfuric acid was purchased from Fisher Scientific. High purity standards (1000 ppm – fluoride, sulfate, nitrate, nitrite) for ion chromatography were purchased from Fluka Analytical, Sigma-Aldrich. Hydrogen peroxide (30%) was purchased from ACROSS Organic, USA. Titanium potassium oxalate dihydrate was purchased from Pfaltz and Bauer. List of all PFAS used in the study is given in Table S1. All materials were used as received. The aqueous solutions were prepared using Milli-Q water (> 20 M Ω cm $^{-1}$ resistivities), generated in-house.

2.2. Sonochemical experiments

Cylindrical coolant jacketed glass reactor was used to conduct sonochemical experiments. The bottom of glass reactor was a flat plate transducer in contact with the solution. The ultrasonic waves of 575 kHz were generated using a multi-frequency generator (model E/805/T/M) and delivered to 200 mL of the sample through a bottom mounted transducer (effective area 22 cm 2). The temperature of the sample was maintained using a refrigerated bath at 21 °C. The initial temperature of the sample was 10 °C which increased to 21 °C in 10 min during sonication and stabilized after that. All experiments were carried out by direct sonication of the sample in an air saturated environment

without sparging air or gas. The calorimetrically measured [29] power intensity (P_I) and power density (P_D) transferred to the solution were 0.69 W/cm 2 and 77 W/L, respectively. A bicomponent solution of PFOA and PFOS, each having an initial concentration range of 0.19 μM –45 μM (0.1 mg/L–20 mg/L), was sonicated. Sonochemical experiments were carried out in duplicates, and error bars show a 95% confidence. Glassware, such as bottles, beakers, and test tubes, were silanized before use. In the silanization process, the glassware was first washed with soapy water, rinsed with hot water, Milli-Q water, rinsed three times with methanol solution and then air dried at 250 °C for 2 h.

A stock solution of PFOA and PFOS (100 mg/L each) was prepared in HPLC grade water. Working solutions of PFOA and PFOS were prepared prior to the experiment by spiking specific volume of the PFAS stock solution into Milli-Q water. A blank control test was performed by spiking PFOA and PFOS in an aqueous solution in the absence of ultrasound irradiation for 3 h. PFAS concentration was unaltered during control experiments.

2.3. Instrumental analysis

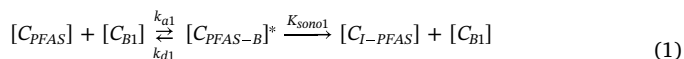
Separation and detection of perfluoroalkyl carboxylic and sulfonic compounds were performed using UPLC coupled with a Xevo TQ-S mass spectrometer (LC/MS/MS, Waters Corp, USA) and a BEH C-18 (2.1 \times 50 mm, 1.7 μm) column (Waters Corp, USA). The mass spectrometer was operated in negative electrospray ionization (ESI $^-$) using multiple reaction monitoring (MRM) mode for each compound (Table S1). The sample injection volume was 10 μL . The column temperature was maintained at 40 °C. The analytes were eluted using HPLC water and acetonitrile mobile phases (Table S2) at a flow rate of 300 $\mu\text{L}/\text{min}$ for 8 min. The electrospray ionization capillary voltage was 3.53 kV with source temperature and desolvation temperatures of 150 °C and 350 °C, respectively. The cone gas flow, desolvation gas flow, and collision gas flow were maintained at 150 L/h, 800 L/h, and 0.14 mL/min, respectively. Laboratory blanks were analyzed during each run. The standard deviation of instrument calibration standards (1–100 $\mu\text{g}/\text{L}$) was less than 20%. Labeled-Isotope surrogates ($^{13}\text{C}_8$ PFOA, $^{13}\text{C}_8$ PFOS) were used. The analytical precision was 5%. The LC/MS/MS instrument limit of detection (LOD) of perfluoroalkyl compounds (C3-C14) and perfluoroalkyl sulfonic compounds (C4, C6, C8) was 1 $\mu\text{g}/\text{L}$ by direct sample injection.

Ion chromatography (IC) analyses of fluoride, nitrite, nitrate, and sulfate were carried out using a Metrohm 930 Compact IC Flex equipped using a Metrosept-A supp 150/4 mm column operating at a flow rate of 0.7 mL/min and a column temperature of 30 °C. The mobile phase was 0.32 M $\text{Na}_2\text{CO}_3/0.1$ M NaHCO_3 . The IC instrument LOD of fluoride, nitrite, nitrate, and sulfate anions was 0.3 mg/L. Hydrogen peroxide was measured using titanium oxalate method [30,31] by measuring the absorbance at 390 nm using a UV-Vis Spectrophotometer. The LOD of hydrogen peroxide was 0.8 mg/L.

3. Sonolytic Michaelis-Menten kinetics model

The Michaelis-Menten model [32] is proposed to model the sonolytic degradation kinetics of perfluoroalkyl substances with the following assumption: (a) active cavity (i.e., cavity taking part in the reaction) acts as a catalyst for PFAS degradation; (b) at a given power density, the cavity collapse forms another collapsible cavity, thus the concentration of active cavities remains constant during the sonolytic reaction; (c) The reaction is irreversible regardless of whether single or multiple products are formed. The development of Michaelis-Menten model for sonolysis is provided in supporting information. Conceptual two-step reaction scheme (Eqs. (1) and (2)) was assumed for sonolytic degradation of PFAS in line with findings of Vecitis et al. (2008) [25] and the present study. The first step involves degradation of PFAS into sono-intermediate of perfluoroalkyl substances, followed by a second step in which PFAS sono-intermediate decompose into an inorganic

constituent of PFAS, such as, fluoride, and sulfate.



where,

$[C_{PFAS}]$ = molar concentration of PFAS;

$[C_{B1}]$ = molar concentration of active cavities which act as a catalyst for sonolytic degradation of PFAS;

$[C_{PFAS-B}]^*$ = molar concentration of active cavity-PFAS complex;

$[C_{I-PFAS}]$ = molar concentration of PFAS-sono-intermediate formed due to decomposition of the active cavity-PFAS complex;

$[C_{B2}]$ = molar concentration of active cavity which act as a catalyst for sonolytic degradation of PFAS-sono-intermediate;

$[C_{I-PFAS-B}]^*$ = molar concentration of active cavity - PFAS-sono-intermediate complex;

$[C_P]$ = molar concentration of final inorganic constituent (fluoride or sulfate) formed due to sonolytic decomposition of the active cavity-PFAS-sono-intermediate complex;

k_{a1} = bimolecular sonolytic association rate constant of the active cavity and PFAS binding, ($\text{mol}^{-1} \text{time}^{-1}$)

k_{d1} = bimolecular sonolytic dissociation rate constant of the active cavity and PFAS complex to regenerate free PFAS, ($\text{mol}^{-1} \text{time}^{-1}$)

k_{sono1} = unimolecular rate constant of the active cavity-PFAS complex to give the free product, and active cavity (time^{-1})

k_{a2} = bimolecular sonolytic association rate constant of the active cavity and PFAS-sono intermediate substance binding, ($\text{mol}^{-1} \text{time}^{-1}$)

k_{d2} = bimolecular sonolytic dissociation rate constant of the active cavity-PFAS-sono intermediate complex to regenerate free PFAS-sono intermediate, ($\text{mol}^{-1} \text{time}^{-1}$)

k_{sono2} = unimolecular rate constant of the active cavity-PFAS-sono intermediate complex to give the free product, and active cavity (time^{-1})

The Turnover rate, ν , for reaction scheme 1 & 2 can be written as follows:

$$\nu_1 = \frac{V_{Max1}[C_{PFAS}]}{K_{M1} + [C_{PFAS}]} \quad (3)$$

$$\nu_2 = \frac{V_{Max2}[C_{I-PFAS}]}{K_{M2} + [C_{I-PFAS}]} \quad (4)$$

where,

$$V_{Max1} = k_{sono1}[C_{B01}], \text{ and } K_{M1} = \left(\frac{k_{d1} + k_{sono1}}{k_{a1}} \right)$$

$$V_{Max2} = k_{sono2}[C_{B02}], \text{ and } K_{M2} = \left(\frac{k_{d2} + k_{sono2}}{k_{a2}} \right)$$

Eqs. (3) and (4) are a fundamental Michaelis-Menten model of a sonolytic reaction kinetics. Here, V_{Max1} and V_{Max2} are the maximum turnover rate when total active cavities participate in the respective reaction scheme. C_{B01} and C_{B02} are molar concentration of total active cavities participating in the respective reaction scheme. K_{M1} and K_{M2} are related to the dissociation constant of the compound bound to the active cavities for reaction (1) and (2), respectively. The method to determine Michaelis-Menten parameters using linear regression and non-linear regression is provided in the [supporting information](#).

4. Results and discussion

Sonolytic degradation of PFOA (Fig. 1a) and PFOS (Fig. 1b) at various initial concentration was monitored along with formation of

fluoride (Fig. 1c), sulfate (Fig. 1d), nitrite (Fig. 2a), nitrate (Fig. 2b), hydrogen peroxide (Fig. 2c), and change in pH (Fig. 2d).

Fig. 1 shows that sonolytic degradation of PFOA and PFOS follows pseudo-first-order reaction kinetics at lower concentrations ($< 2.34 \mu\text{M}$) and zero-order kinetics at higher concentrations. Likewise, the sonochemical formation of fluoride and sulfate followed zero-order kinetics. The degradation kinetics, as shown in Fig. 3 (zero order, i.e., initial rate) and Fig. 4a (pseudo first order), are lower than previously reported values in the literature [10–12,33]. This is due to lower ultrasound power density (77 W L^{-1}) and power intensity (0.69 W cm^{-2}) in this study compared to 250 W L^{-1} and 6.4 W cm^{-2} used by Vecitis et al. (2008) [11] for a similar initial concentration ($20 \mu\text{M}$) of PFOA and PFOS. Fig. 3 shows that degradation of PFOA and PFOS, as well as the formation of fluoride anions and sulfate anions, follows saturation kinetics. These results are in agreement with the previously reported results in the literature [11,33]. The observed saturation kinetics is similar to the enzyme-catalyzed kinetics. Perfluoroalkyl carboxylic compounds (carbon chain length: C3-C7, C9-C14, C16, and C18) and perfluoroalkyl sulfonic compounds (chain length: C4, C6) were not detected during analysis. The absence of short-chain PFAS during degradation of PFOA and PFOS suggests that the sonolytic reactions do not follow step by step electron transfer pathway as in sulfate radical [34] or photocatalytic [35] degradation processes.

Over a range of PFOS concentration, the rate of sulfate ion formation was $12\text{--}26 \text{ nM/min}$ and rate of degradation of sulfur-containing PFOS were $25\text{--}54 \text{ nM/min}$ (Fig. 3). These results correspond to the mineralization of approximately 50% of PFOS to sulfate anions at a given concentration and time. Fig. 1b and d show that corresponding mass balance of formation of sulfate anions and PFOS degradation is less than one. These results are in agreement with the results obtained by Rodriguez-Freire et al. [33]. However, these results are in contrast with Vecitis et al. [25], wherein, it was hypothesized that C-S cleavage of PFOS is the first step for degradation of PFOS.

If the concentration of the surfactant is above critical micelle concentration (CMC), the hydrophobic part of surfactant “hides” itself inside the micelle and hydrophilic part is oriented towards the aqueous environment [36]. Thus, the fluorinated hydrophobic tail of PFAS will be first to get exposed to an elevated temperature at the cavity-water interfacial region during cavity collapse. If the PFAS concentration is below CMC, surface tension decreases with increase in PFAS concentration. Moreover, adsorption at the air-water interface is diffusion controlled [37]. This suggests that structural orientation of all PFAS molecules adsorbed to air-water interface might not be identical when PFAS concentration is below CMC. The concentration of PFAS ($< 87 \mu\text{M}$) in the present study is much lower than the reported CMC values of PFOA (8 mM) & PFOS (8 mM) [2,37]. Thus, the first step of sonolytic degradation of PFAS might depend on the structural orientation of PFAS at cavity water interface at the time of PFAS-cavity adsorption, i.e., whether fluorinated hydrophobic tail or hydrophilic (carboxylic or sulfonate) tail is oriented toward the active cavity-water interface. Hence, pyrolytic C-S bond cleavage of PFOS or cleavage of an ionic head group of PFAS may not be the initial step for sonolytic decomposition of PFAS.

Likewise, the corresponding mass balance of formation of fluoride ion and the degradation of a mixture of PFOA and PFOS was less than 1 (Fig. 1). It was observed that 60%–80% of the fluoride ion was accounted from the degraded mixture of PFOA and PFOS at any point during sonochemical decomposition. Fig. 4a shows that pseudo-first-order constant of degradation of PFOA and PFOS decreases with an increase in the initial concentration of PFAS. On the contrary, the variation of the pseudo-first-order constant of formation of fluoride ion ($0.014 \pm 9\% \text{ min}^{-1}$) and sulfate ion ($0.0093 \pm 6\% \text{ min}^{-1}$) is insignificant. These results suggest that sonochemical degradation follows sequential steps, where PFAS first forms intermediate byproduct (i.e., PFAS-sono-intermediate), which subsequently get mineralized into fluoride and sulfate ions. These results are in agreement with Vecitis

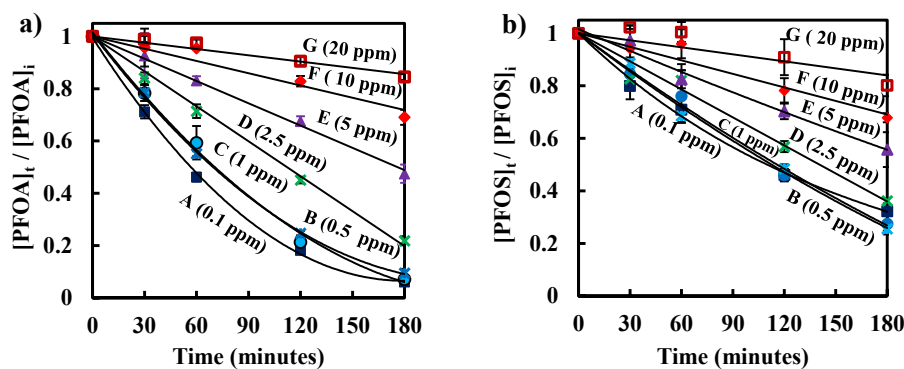


Fig. 1. Degradation of (a) PFOA, (b) PFOS and formation of (c) fluoride anion, (d) sulfate anion over a range of initial concentration under sonolytic conditions: 575 kHz, 77 W/L, 0.69 W/cm², 200 mL, Temp_i = 10 °C, Temp_f = 21 °C; [A: (■), [PFOA]_i = 0.2 μM, [PFOS]_i = 0.25 μM; B: (●), [PFOA]_i = 1.09 μM, [PFOS]_i = 1.3 μM; C: (×), [PFOA]_i = 2.34 μM, [PFOS]_i = 2.78 μM; D: (×), [PFOA]_i = 5.44 μM, [PFOS]_i = 7.38 μM; E: (▲), [PFOA]_i = 10.85 μM, [PFOS]_i = 14.59 μM; F: (◆), [PFOA]_i = 23.60 μM, [PFOS]_i = 29.48 μM; G: (□), [PFOA]_i = 41.61 μM, [PFOS]_i = 45.45 μM] (Error bar shows 95% confidence interval).

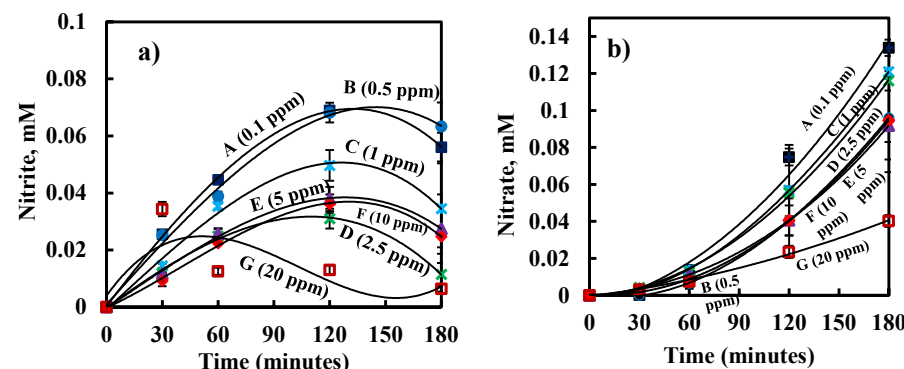
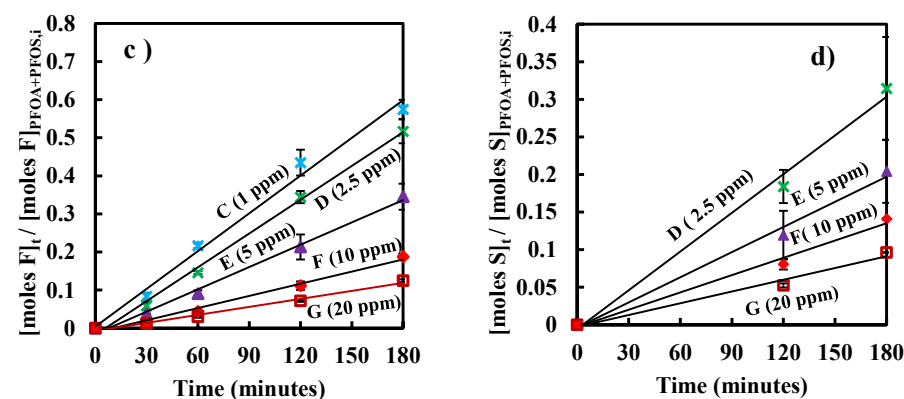
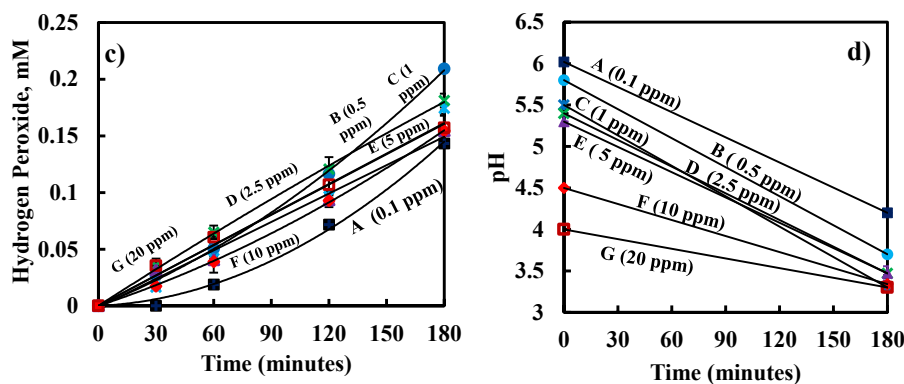


Fig. 2. Formation of (a) Nitrite, (b) Nitrate, (c) Hydrogen peroxide and (d) pH variation during sonolytic degradation of mixture of PFOA and PFOS [A: (■), [PFOA]_i = 0.2 μM, [PFOS]_i = 0.25 μM; B: (●), [PFOA]_i = 1.09 μM, [PFOS]_i = 1.3 μM; C: (×), [PFOA]_i = 2.34 μM, [PFOS]_i = 2.78 μM; D: (×), [PFOA]_i = 5.44 μM, [PFOS]_i = 7.38 μM; E: (▲), [PFOA]_i = 10.85 μM, [PFOS]_i = 14.59 μM; F: (◆), [PFOA]_i = 23.60 μM, [PFOS]_i = 29.48 μM; G: (□), [PFOA]_i = 41.61 μM, [PFOS]_i = 45.45 μM] (Error bar shows 95% confidence interval).



337

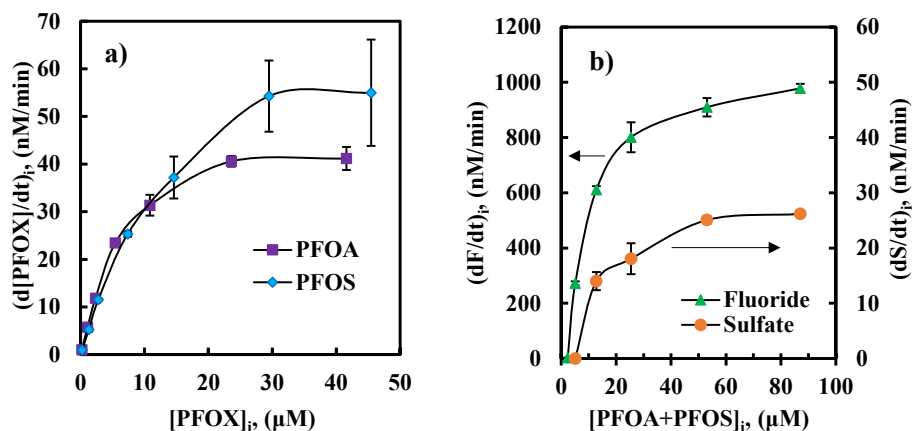


Fig. 3. Initial rate of (a) degradation of PFOA and PFOS (b) formation of fluoride and sulfate during sonolytic degradation of mixture of PFOA and PFOS (PFOX is the representative sulfonate or carboxylate concentration where X = A or S).

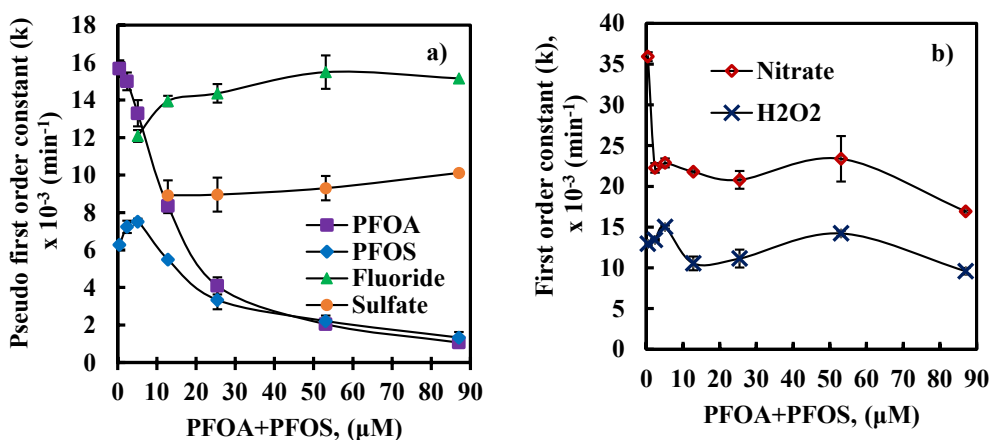


Fig. 4. (a) Pseudo-first-order rate constant of degradation of PFOA, PFOS, and formation of fluoride and sulfate (b) first-order rate constant of formation of nitrate and hydrogen peroxide.

Table 1
Michaelis-Menten kinetic parameter obtained using linear and nonlinear regressions.

Compound	Parameter	Linear Regression			Non-linear Regression	
		L-B Method	H-W Method	E-H Method	Excel – SOLVER Method	MATLAB Method
PFOA	V_{max} (nM min ⁻¹)	102	50	54	50	50
	K_m (μM)	19.70	7.60	8.86	6.55	6.55
	R^2	1.00	0.99	0.90	–	–
	SSR	1034	18	24	10.40	10.38
PFOS	V_{max} (nM min ⁻¹)	663.59	80.01	82.59	75.94	75.94
	K_m (μM)	179.12	17.69	18.59	14.68	14.67
	R^2	1.00	0.98	0.89	–	–
	SSR	8020	29	31	20	20
Fluoride	V_{max} (nM min ⁻¹)	1359	1130	1178	1135	1135
	K_m (μM)	19.84	12.73	14.42	12	12
	R^2	0.98	1.00	0.06	–	–
	SSR	30,485	7123	8363	6543	6552
Sulfate	V_{max} (nM min ⁻¹)	31.05	31.52	31.40	31.90	31.90
	K_m (μM)	15.97	16.60	16.41	17	17
	R^2	0.98	1.00	0.95	–	–
	SSR	2.51	2.31	2.35	2	2

SSR = Residual Sum of Squared, R^2 = Coefficient of determination, L-B = Lineweaver-Burk plot method; H-W: Hanes-Woolf plot method; E-H: Eadie-Hofstee plot method.

et al. [25] findings and indicate that sonochemical degradation of PFOA and PFOS follows multiple, sequential pyrolytic steps.

Over the range of PFAS concentration, the half-life of PFOA and PFOS decomposition ranged from 44 min to 651 min, on the contrary, corresponding half-life of fluoride and sulfate formation was 49 ± 4.5 min and 75 ± 3.6 min respectively. The ratio of the pseudo-first-order rate constant of sulfate to sulfate-containing PFOS increases from 1.6 to 7.6 with an increase in the concentration of PFOS from $0.25 \mu\text{M}$ to $29.5 \mu\text{M}$. Similarly, the ratio of the pseudo-first-order rate constant of fluoride to PFOA and PFOS combined increases from 0.5 to 3.6 with an increase in the concentration of PFAS (Fig. 4a). Further, insignificant change in pseudo-first-order rate constant of formation of fluoride & sulfate suggests that the rate of degradation of PFAS-sono-intermediate into PFAS inorganic compound is constant over a range of concentration. These results indicate that at higher PFAS concentration, the rate of degradation of PFAS-sono-intermediate to fluoride & sulfate is higher than the rate of degradation of PFAS to PFAS-sono-intermediate. Besides, sonochemical degradation of PFAS into PFAS-sono-intermediate is a function of adsorption of PFAS at the cavity-water interface during cavity collapse. Thus, it can be postulated that the adsorption of PFAS on the cavity-water interface through diffusion is the rate-limiting step in the sonochemical reaction.

The ratio of the pseudo-first-order rate constant of PFOA and PFOS was 2.4 at a lower PFAS concentration ($0.45 \mu\text{M}$) and decreased to 0.79 at a higher PFAS concentration ($87 \mu\text{M}$). Thus, as shown in Fig. 4a, PFOA has higher degradation compared to PFOS at a lower PFAS concentration ($< 25.43 \mu\text{M}$). But, PFAS degradation follows zero order kinetics at a higher PFAS concentration ($> 25.43 \mu\text{M}$) and the ratio of the zero-order constant of PFOS and PFOA increases from 1.08 to 1.34 with an increase in concentration from $25.43 \mu\text{M}$ to $87 \mu\text{M}$. Thus, as shown in Fig. 3a, PFOS has slightly higher degradation rate compared to PFOA at higher PFAS concentration.

The sonochemical initial rate of degradation of PFAS was modeled using Michaelis-Menten Model. Table 1 shows Michaelis-Menten model parameters of sonochemical degradation of PFOA and PFOS, and formation of fluoride and sulfate obtained using linear regression and non-linear regression methods described in supporting information. The initial rates were plotted as a function of PFAS concentration, fitted by Michaelis-Menten kinetic parameters (Fig. 6). It may be observed that all methods provide an excellent fit to the data except Lineweaver-Burk plot method. F-test for best curve fitting model given in Table S3 (Supporting Information) shows that Hanes-Woolf plot is best fit method among linear regression and both Excel-Solver and MATLAB method for non-linear regression give best curve fitting parameter over all.

Pseudo-first-order kinetics of the PFOA and PFOS as a function of concentration was modeled using power law as shown in Fig. 7. Modeled equation obtained for sonochemical degradation of PFOA and PFOS, and formation of fluoride and sulfate are as given in Table 2. The lower residual sum of squares (SSR) indicates the statistically significant relationship between modeled pseudo-first-order rate constant (k_m) value and experimental pseudo-first-order rate constant (k) values. No attempt was made to define the physical relationship of a coefficient obtained through the power law equation with sonochemical reactions. Thus, the power law is solely used for describing the statistical relationship between the concentration of PFAS and pseudo-first-order

Table 2
Modeled power law rate equation for pseudo-first-order constant.

Compound	Modeled power law equation	R ²	SSR
PFOA	$k = 0.325[C_{\text{PFOA}}]^{-0.889}$	0.99	5.16
PFOS	$k = 0.016[C_{\text{PFOS}}]^{-0.61}$	0.96	1.83
Fluoride	$k = 0.0109[C_{\text{PFOA}} + C_{\text{PFOS}}]^{0.0823}$	0.89	8.46
Sulfate	$k = 0.0073[C_{\text{PFOA}} + C_{\text{PFOS}}]^{0.068}$	0.89	12.1

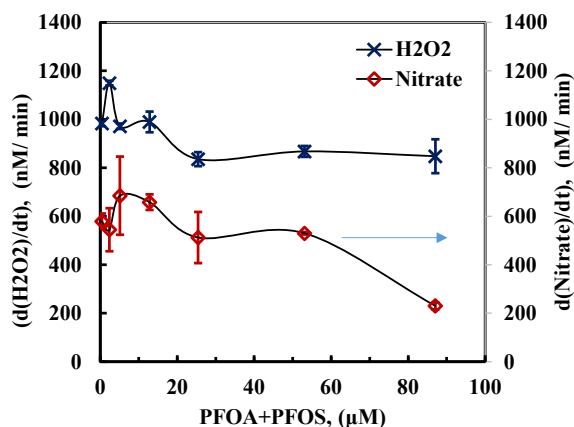


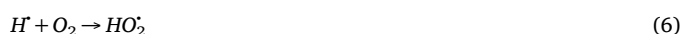
Fig. 5. Rate of formation of hydrogen peroxide and nitrate during sonochemical degradation of mixture of PFOA and PFOS.

constant and limited to the condition of the study. However, as described in the subsequent paragraph, the power law relationship is utilized to determine the pseudo-first order rate constant (k_{sono}) of sonochemical reaction, when $v = V_{\text{Max}}$.

4.1. Nitrite, nitrate and hydrogen peroxide formation

Fig. 2 shows the formation of nitrite, nitrate, and hydrogen peroxide during sonochemical degradation of a mixture of PFOA and PFOS. Nitrite concentration increased during the initial 120 min of sonication and, then started decreasing, and finally seem stabilized. On the other hand, the concentration of nitrate increased exponentially after 60 min. This pattern suggests a sequential sonochemical conversion of atmospheric nitrogen into nitrite and subsequently into nitrate. The observation of nitrate formation agrees with the results reported previously in the literature [31,38]. The exponential time-dependent increase in the concentration of nitrate indicates its accumulation in the solution as a final sonochemical byproduct of the process.

Over a range of PFAS concentration, the average first-order rate constant of the formation of nitrate and hydrogen peroxide is $0.0234 (\pm 23\%) \text{ min}^{-1}$ ($t_{1/2} = 30$ min) and $0.0124 (\pm 15\%) \text{ min}^{-1}$ ($t_{1/2} = 54$ min), respectively (Fig. 4b). Further, as shown in Fig. 5, the average rate of formation of hydrogen peroxide and nitrate was $0.949 \pm 0.11 \mu\text{M}/\text{min}$ (RSD: 10%) and $0.534 \pm 0.14 \mu\text{M}/\text{min}$ (RSD: 25%), respectively. These results indicate an insignificant effect of PFAS concentration on the sonochemical formation of hydrogen peroxide. There was a 71% decrease in nitrate formation with an increase in PFAS concentration from $0.4 \mu\text{M}$ to $87 \mu\text{M}$ (Fig. 2b) along with the corresponding reduction in nitrite formation (Fig. 2a). There was 37% drop in first-order rate constant of nitrate formation with increase in PFAS concentration from $0.4 \mu\text{M}$ to $2.4 \mu\text{M}$ (Fig. 4b). This indicates that higher PFAS concentration has a significant effect on nitrate formation kinetics. At higher PFAS concentration, there is higher adsorption of PFAS molecules on the cavity-water interface, and which restricts the diffusion of atmospheric nitrogen and oxygen into the cavity leading to lower pyrolytic conversion of nitrogen gas into nitrite and nitrate. However, the adsorption of PFAS on the cavity-water interface has an insignificant effect on the formation of hydrogen peroxide. It can be inferred that sufficient water vapors and oxygen was available in the core of the cavity during collapse for pyrolytic conversion of water vapor into hydrogen peroxide via radical species as shown in Eqs. (5)–(8) [13].



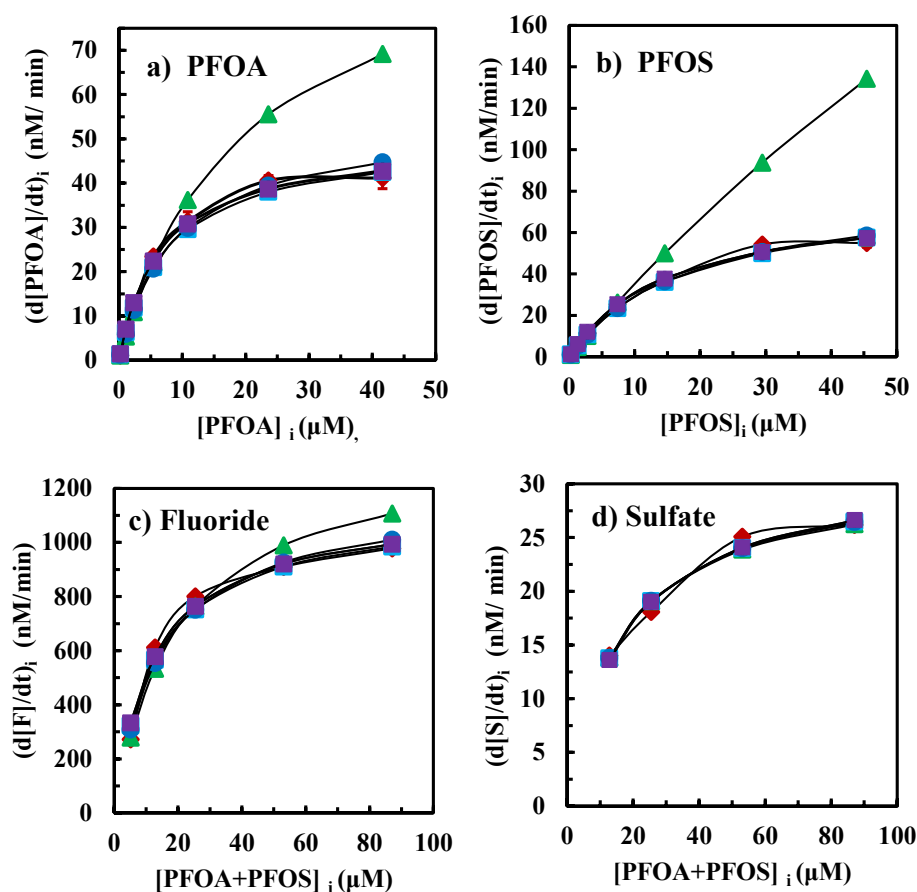


Fig. 6. Initial rate of (a) PFOA degradation (b) PFOS degradation (c) Fluoride formation (d) Sulfate formation plotted as a function of PFAS concentration fitted by Michaelis-Menten kinetic model. (♦): Experimental; (▲): L-B Method; (■): H-W Method; (●): E-H Method; (+): Excel-SOLVER Method; (×): Matlab Method.



The rate of formation of nitrate is 0.6 times lower than that of hydrogen peroxide (Fig. 5) over the range of PFAS concentration. The bond dissociation energy (at 298 K) of N–N bond (945 kJ/mol) is higher than O–O bond (498 kJ/mol), H–F bond (569.87 kJ/mol), H–H bond (435.9 kJ/mol) and H–O bond (429 kJ/mol) [39]. Consequently, nitrogen gas requires higher temperature compared to oxygen and water vapor to dissociate into its atomic states during the collapse of the cavity. Dissociation of oxygen, nitrogen, and water vapor occurs at the core of the cavity during the violent collapse. These compounds also cushion adiabatic collapse of the cavity and generate reduced thermal shock and temperature during the collapse. Thus, it can be inferred that a limited number of cavity collapse occurs which generate sufficient temperature (above 1600 °C) to dissociate nitrogen gas. These dissociate nitrogen gas radicals ultimately forms nitrite and nitrate due to subsequent sonolytic reactions. Thus, it can be deduced that a number of cavity collapse which generates temperature sufficient to dissociate water vapor and oxygen are approximately equal to or more than 1.6 times higher than numbers of cavity collapse which dissociate nitrogen gas.

Figs. 3b and 5 shows that rate of fluoride formation (0.97 μM/min) at a PFAS concentration of 87 μM is similar to the average rate of hydrogen peroxide formation (0.95 μM/min). The bond dissociation energy of the O–O bond (498 kJ/mol), H–O bond (429 kJ/mol), and C–F bond (552 kJ/mol) are almost in the same range [39]. This indicates that parent compounds of fluoride and hydrogen peroxide are exposed to identical temperature environment during cavity collapse. C–F bond breakage of PFAS occurs at interfacial region of the collapsible cavity due to a PFAS preference for the air-water interface. Thermal decomposition of PFOA & PFOS at elevated temperature (350–700 °C) is reported in the literature. [28,40]. These results suggest that collapse of

cavity generate a temperature of more than 350 °C at the interfacial region of the collapsing cavity.

Fig. 2d shows the drop in initial pH of PFAS to less than 4.7 over a range of concentration. Increase in PFAS concentration decreased the pH during the sonolytic reaction. The formation of hydrogen fluoride may be one of the reasons for the drop in pH. But, formation of hydrogen peroxide which is weak acid; formation of nitric acid or nitrous acid due to reaction between hydrogen peroxide, water, and nitrogen radical species [13]; formation of carbonic acid due to reaction of carbon dioxide with radical species [13], and formation unknown PFAS-sono-intermediate might also decrease pH of the solution.

4.2. Estimation of active cavities concentration

The maximum concentration of active cavities (i.e., those taking part in the reaction) (C_{Bo}) generated during sonolysis and having a minimum energy sufficient to degrade a given compound can be calculated using equation (9) (from Eq. (S12)),

$$[C_{Bo}] = \frac{V_{Max}}{k_{sono}} \quad (9)$$

Similarly, Michaelis-Menten kinetics relationship can be used to determine the concentration of PFAS required to achieve maximum turnover rate (V_{Max}) i.e., the minimum concentration of PFAS at which $v = V_{Max}$. The pseudo-first-order rate constant (k_{sono}) when $v = V_{Max}$ can be calculated using power law relationships (Table 2). Estimated values of concentration of PFAS, k_{sono} and C_{Bo} , when the turnover rate of the ultrasonic system is maximum, i.e when $v = V_{Max}$ are listed in Table 3.

The active cavity sites for reaction with PFOA & PFOS were 89.25 mM and 8.8 mM respectively. These active cavities have more probability of transforming the PFAS-cavity complex into PFAS-sono-intermediate byproducts. Cavity sites participating in the degradation

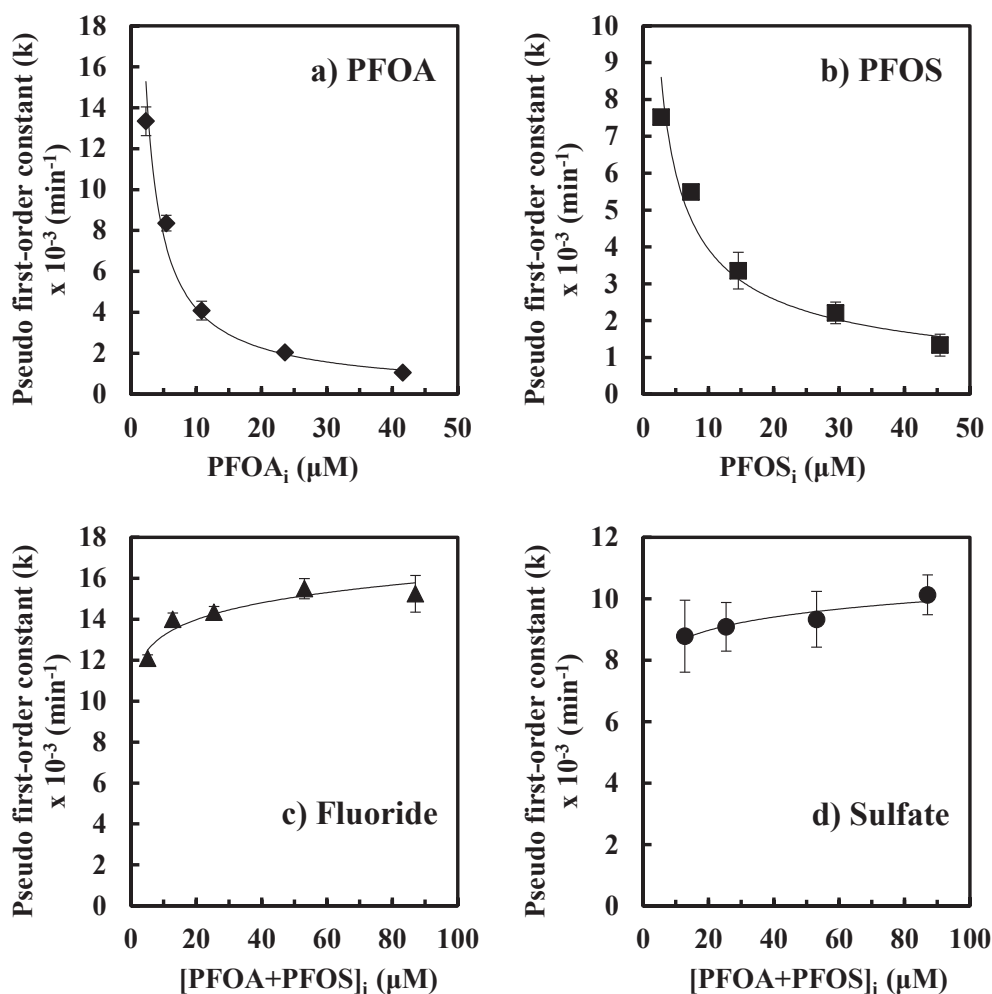


Fig. 7. Pseudo-first order rate constant of (a) PFOA (b) PFOS (c) Fluoride (d) Sulfate plotted as a function of PFAS concentration fitted by power law model (Error bar shows 95% confidence interval of experimental data).

Table 3

Estimated values of PFAS concentration, turnover rate, k_{sono} , C_{Bo} , and sonolytic efficiency when turnover rate is equal to V_{Max} .

Attribute	Unit	PFOA	PFOS	Fluoride	Sulfate
$[C_{PFAS}]$	mM	23	23	46	46
Turnover rate, v	nM min ⁻¹	50	76	1135	32
k_{sono}	min ⁻¹	5.56E-07	8.58E-06	3.19E-02	1.77E-2
$[C_{Bo}]$	mM	89.25	8.8	0.0356	0.0018
$\frac{k_{sono}}{k_M}$	M ⁻¹ min ⁻¹	0.85	5.84	25,873	10,271

of PFOA are approximately 10 times higher than that for PFOS. The bond dissociation energy of the C–S bond (714.1 kJ/mol) is higher than a C–C bond (610 kJ/mol) [39]. Thermal degradation of sulfonate group occurs at temperature 100–200 °C higher compared to thermolytic decomposition of the corresponding carboxylic group [25,28,40]. This suggests that PFOS needs at least 100–200 °C higher temperature compared to PFOA for its thermolytic degradation. Thus, it can be inferred that the ultrasonic system generates a lower number of cavity collapse with temperature sufficient to degrade PFOS compared to the cavity collapse with temperature which degrades PFOA. The lower specificity constant of PFOA ($0.85 \text{ M}^{-1} \text{ min}^{-1}$) compared to PFOS ($5.84 \text{ M}^{-1} \text{ min}^{-1}$) indicates that the cavity-water interface has a lower affinity for PFOA compared to PFOS. This property of PFAS is in agreement with the air-water interface theory of surfactant [36].

At lower PFAS concentration ($< 5.12 \mu\text{M}$), PFAS degradation

follows pseudo-first-order kinetics (Fig. 1a and b) and Fig. 4 shows that the pseudo-first-order rate constant of PFOA is higher compared to PFOS. This result suggests that PFOA degrades faster compared to PFOS at lower initial PFAS concentration. The ultrasonic system generates a lower number of cavity collapse which degrades PFOS compared to PFOA. Thus, the probability of diffusion of PFOS molecules on collapsible cavity-water interface reduces due to a lower number of PFOS molecules and lower number of collapsible cavity compared to PFOA. This may be the reason for lower PFOS degradation compared to PFOA at lower PFAS concentration.

At higher PFAS concentration ($> 5.12 \mu\text{M}$), more PFOS molecules are available for adsorption at the cavity-water interface. Further, seven times greater affinity (specificity constant, $\frac{k_{sono}}{k_M}$) of an active cavity for PFOS adsorption compared to PFOA, increases the probability of PFOS adsorption to collapsible cavity even though the concentration of active cavities for PFOS is 10 times lower than PFOA. This could be the reason for slightly higher degradation rate of PFOS when compared to that of PFOA at higher initial PFAS concentration.

The sonolytic degradation follows sequential degradation of PFAS first into PFAS-sono-intermediate and then degradation of PFAS-sono-intermediate into PFAS inorganic compounds. Formation of PFAS-sono-intermediate occurs at the interfacial region of the collapsible cavity. PFAS-sono-intermediate depending on its Henry's constant and solubility might diffuse into the core of collapsible cavity, adsorb on the cavity-water interface or dissolve in the bulk solution. Thus, degradation of PFAS-sono-intermediate could occur a) in the core of collapsible

cavity if PFAS-sono-intermediate is highly volatile, b) on the interfacial region if sono-intermediate are non-volatile c) or in the bulk solution with highly reactive radicals generated due to cavity collapse. Lower C_{Bo} values for the formation of fluoride and sulfate compared to PFOA and PFOS indicate lower the dependence of cavity-PFAS-sono-intermediate complex degradation on active cavities for further degradation. In this case, the reaction may be mostly driven by very high-temperature thermolytic decomposition inside the core of active cavity during cavity collapse as demonstrated by Vecitis et al. (2008) [25] or it could be due to the reaction of the intermediate complex with highly reactive radicals in bulk water.

Ultrasonic irradiation of aqueous solution creates many cavities in the sample. Very few cavities generate elevated temperature in the core of cavity and on the cavity-water interface during the collapse. A considerable number of cavities generate lower temperature during the collapse and may not be useful for PFAS degradation. Thus, the present study suggests that the ultrasonic system generates a limited number of cavities that could participate in the thermolytic conversion of highly stable compounds such as PFAS. Consequently, it can be inferred that, at certain applied ultrasound frequency and amplitude, sonochemical kinetics primarily depends on a total number of cavity events per unit time that generate sufficient temperature after the collapse and there is the proximity of chemical to the elevated temperature.

5. Conclusions

Sonolytic degradation of non-volatile surfactant perfluoroalkyl carboxylic acid and perfluoroalkyl sulfonic acid is a function of adsorption of the PFAS at the cavity-water interface, and it follows saturation kinetics. Over a range of PFAS concentration, the half-life of degradation of PFOA and PFOS ranged from 44 to 651 min whereas half-life of formation of fluoride and sulfate was 49 min and 75 min respectively at an ultrasonic frequency of 575 kHz and power density of 77 W/L. This suggests that adsorption of PFAS on the cavity-water interface is rate limiting step for ultrasonic degradation of PFAS. The study indicates that cleavage of an ionic head group of the perfluoroalkyl substance is not the first step of sonolytic degradation and it might be dependent on the structural orientation of PFAS at the time of adsorption at the cavity-water interface. The rate of formation of hydrogen peroxide and nitrate was 0.949 $\mu\text{M}/\text{min}$ (RSD: 10%) and 0.534 $\mu\text{M}/\text{min}$ (RSD: 25%) over a range of PFAS concentration. Increase in PFAS concentration decreased the nitrate formation. However, no significant difference in hydrogen peroxide formation observed. Nitrate accumulates as a final byproduct during sonolytic degradation of PFAS. Maximum turnover rate estimated using Michaelis-Menten kinetics and pseudo-first-order of sonolytic transformation modeled using power law can be utilized to estimate maximum active cavities participated in the reaction for non-volatile surfactant such as perfluoroalkyl substances. The estimated maximum turnover rate (V_{max}) for PFOA and PFOS degradation rate is 49 nM min^{-1} and 75 nM min^{-1} respectively, whereas, maximum fluoride and sulfate formation rate is 1135 nM min^{-1} and 31 nM min^{-1} . The estimated maximum concentration of active cavities participated during the process are 89.25 mM, 8.8 mM, 0.036 mM, and 0.0018 mM for PFOA, PFOS, fluoride, and sulfate respectively. Thus, though PFOS has maximum surface activity, the lower degradation rate of PFOS compared to PFOA at lower concentration is due to lower numbers of collapsible cavities with elevated temperature. The ultrasonic system generates very few cavity collapses which can generate elevated temperature at the core and on the cavity interfacial region for degradation of PFAS and formation of nitrate from nitrogen gas. The degradation of dilute PFAS contaminated water using high-frequency ultrasound seems viable methods due to faster mineralization rate of PFAS into its inorganic compounds. However, further investigation is needed on the effect of ultrasonic process parameters such as power density, bulk water temperature, gases, reactor design, frequency, and environmental matrix which may affect energy requirements and

degradation kinetics. Machalies-Menten Model was able to describe the sonolytic degradation of perfluoroalkyl substance and helped to understand adsorption behavior of PFAS at the cavity-water interface.

Acknowledgments

This research was supported by the National Science Foundation (NSF) – Water and Environmental Technology (WET) Center at Temple University. Opinions, findings, and conclusions expressed in this paper are those of the authors and do not necessarily reflect the views of NSF, WET Center or Temple University.

Appendix A. Supplementary data

Supplementary data associated with this article can be found, in the online version, at <https://doi.org/10.1016/j.ultsonch.2018.08.028>.

References

- [1] R.C. Buck, J. Franklin, U. Berger, J.M. Conder, I.T. Cousins, P. De Voogt, A.A. Jensen, K. Kannan, S.A. Mabury, S.P.J. van Leeuwen, Perfluoroalkyl and polyfluoroalkyl substances in the environment: terminology, classification, and origins, *Integr. Environ. Assess. Manage.* 7 (2011) 513–541, <https://doi.org/10.1002/ieam.258>.
- [2] S. Rayne, K. Forest, Perfluoroalkyl sulfonic and carboxylic acids: a critical review of physicochemical properties, levels and patterns in waters and wastewaters, and treatment methods, *J. Environ. Sci. Health Part A* 44 (2009) 1145–1199, <https://doi.org/10.1080/10934520903139811>.
- [3] A.L. Myers, P.W. Crozier, P.A. Helm, C. Brimacombe, V.I. Furdui, E.J. Reiner, D. Burniston, C.H. Marvin, Fate, distribution, and contrasting temporal trends of perfluoroalkyl substances (PFASs) in Lake Ontario, Canada, *Environ. Int.* 44 (2012) 92–99, <https://doi.org/10.1016/j.envint.2012.02.002>.
- [4] A. Urtiaga, C. Fernández-González, S. Gómez-Lavín, I. Ortiz, Kinetics of the electrochemical mineralization of perfluorooctanoic acid on ultrananocrystalline boron doped conductive diamond electrodes, *Chemosphere* 129 (2015) 20–26, <https://doi.org/10.1016/j.chemosphere.2014.05.090>.
- [5] J. Niu, Y. Li, E. Shang, Z. Xu, J. Liu, Electrochemical oxidation of perfluorinated compounds in water, *Chemosphere* 146 (2016) 526–538, <https://doi.org/10.1016/j.chemosphere.2015.11.115>.
- [6] S.C. Panchangam, A.Y. Lin, K.L. Shaik, C. Lin, Decomposition of perfluorocarboxylic acids (PFCAs) by heterogeneous photocatalysis in acidic aqueous medium, *Chemosphere* 77 (2009) 242–248, <https://doi.org/10.1016/j.chemosphere.2009.07.003>.
- [7] Y.C. Lee, S.L. Lo, J. Kuo, Y.L. Lin, Persulfate oxidation of perfluorooctanoic acid under the temperatures of 20–40 °C, *Chem. Eng. J.* 198–199 (2012) 27–32, <https://doi.org/10.1016/j.cej.2012.05.073>.
- [8] N. Merino, Y. Qu, R.A. Deeb, E.L. Hawley, M.R. Hoffmann, S. Mahendra, Degradation and removal methods for perfluoroalkyl and polyfluoroalkyl substances in water, *Environ. Eng. Sci.* 33 (2016) 615–649, <https://doi.org/10.1089/ees.2016.0233>.
- [9] T.Y. Campbell, M.R. Hoffmann, Sonochemical degradation of perfluorinated surfactants: power and multiple frequency effects, *Sep. Purif. Technol.* 156 (2015) 1019–1027, <https://doi.org/10.1016/j.seppur.2015.09.053>.
- [10] H. Moriwaki, Y. Takagi, M. Tanaka, K. Tsuruho, O. Kenji, Y. Maeda, Sonochemical decomposition of perfluorooctane sulfonate and perfluorooctanoic acid, *Environ. Sci. Technol.* 39 (2005) 3388–3392, <https://doi.org/10.1021/es040342v>.
- [11] C.D. Vecitis, H. Park, C. Jie, B.T. Mader, M.R. Hoffmann, Enhancement of perfluorooctanoate and perfluorooctanesulfonate activity at acoustic cavitation bubble interfaces, *J. Phys. Chem. C* 112 (2008) 16850–16857, <https://doi.org/10.1021/jp804050p>.
- [12] N.A. Fernandez, L. Rodriguez-Freire, M. Keswani, R. Sierra-Alvarez, Effect of chemical structure on the sonochemical degradation of perfluoroalkyl and polyfluoroalkyl substances (PFASs), *Environ. Sci. Water Res. Technol.* 2 (2016) 975–983, <https://doi.org/10.1039/C6EW00150E>.
- [13] Yusuf G. Adewuyi, Sonochemistry: environmental science and engineering applications, *Ind. Eng. Chem. Res.* 40 (2001) 4681–4715, <https://doi.org/10.1021/ie010096l>.
- [14] G. Andaluri, E.V. Rokhina, R.P.S. Suri, Evaluation of relative importance of ultrasound reactor parameters for the removal of estrogen hormones in water, *Ultrason. Sonochem.* 19 (2012) 953–958, <https://doi.org/10.1016/j.ultsonch.2011.12.005>.
- [15] R.P.S. Suri, M. Nayak, U. Devaiah, E. Helmig, Ultrasound assisted destruction of estrogen hormones in aqueous solution: effect of power density, power intensity and reactor configuration, *J. Hazard. Mater.* 146 (2007) 472–478, <https://doi.org/10.1016/j.jhazmat.2007.04.072>.
- [16] R.P.S. Suri, A. Kamrajapuram, H. Fu, Ultrasound destruction of aqueous 2-chlorophenol in presence of silica and peroxide, *Environ. Eng. Sci.* 25 (2008) 1447–1454, <https://doi.org/10.1089/ees.2007.0145>.
- [17] Y.T. Didenko, W.B. McNamara III, K.S. Suslick, Hot spot conditions during cavitation in water, *J. Am. Chem. Soc.* 121 (1999) 5817–5818, <https://doi.org/10.1021/ja9844635>.

- [18] W.B. McNamara III, Y.T. Didenko, K.S. Suslick, Sonoluminescence temperatures during multi-bubble cavitation, *Nature* 401 (1999) 772–775, <https://doi.org/10.1038/44536>.
- [19] E.B. Flint, K.S. Suslick, The temperature of cavitation, *Science* (80-) 253 (1991) 1397–1399, <https://doi.org/10.1126/science.253.5026.1397>.
- [20] M. Ashokkumar, T.J. Mason, Sonochemistry, *Kirk-Othmer Encycl. Chem. Technol.* (2000) 353–372, <https://doi.org/10.1002/0471238961.1915141519211912.a01>.
- [21] R. Tronson, M. Ashokkumar, F. Grieser, Multibubble sonoluminescence from aqueous solutions containing mixtures of surface active solutes, *J. Phys. Chem. B* 107 (2003) 7307–7311, <https://doi.org/10.1021/jp034360v>.
- [22] D. Sunartio, M. Ashokkumar, F. Grieser, Study of the coalescence of acoustic bubbles as a function of frequency, power, and water-soluble additives, *J. Am. Chem. Soc.* 129 (2007) 6031–6036, <https://doi.org/10.1021/ja068980w>.
- [23] J.Z. Sostaric, P. Riesz, Adsorption of surfactants at the gas/solution interface of cavitation bubbles: an ultrasound intensity-independent frequency effect in sonochemistry, *J. Phys. Chem. B* 106 (2002) 12537–12548, <https://doi.org/10.1021/jp022106h>.
- [24] M. Chiha, S. Merouani, O. Hamdaoui, S. Baup, N. Gondrexon, C. Pétrier, Modeling of ultrasonic degradation of non-volatile organic compounds by Langmuir-type kinetics, *Ultrason. Sonochem.* 17 (2010) 773–782, <https://doi.org/10.1016/j.ultrasonch.2010.03.007>.
- [25] C.D. Vecitis, H. Park, J. Cheng, B.T. Mader, M.R. Hoffmann, Kinetics and mechanism of the sonolytic conversion of the aqueous perfluorinated surfactants, perfluorooctanoate (PFOA), and perfluorooctane sulfonate (PFOS) into inorganic products, *J. Phys. Chem. A* 112 (2008) 4261–4270, <https://doi.org/10.1021/jp801081y>.
- [26] A. Guiseppi-Elie, S.H. Choi, K.E. Geckeler, Ultrasonic processing of enzymes: effect on enzymatic activity of glucose oxidase, *J. Mol. Catal. B: Enzyme* 58 (2009) 118–123, <https://doi.org/10.1016/j.molcatb.2008.12.005>.
- [27] P.B. Subhedar, P.R. Gogate, Enhancing the activity of cellulase enzyme using ultrasonic irradiations, *J. Mol. Catal. B: Enzyme* 101 (2014) 108–114, <https://doi.org/10.1016/j.molcatb.2014.01.002>.
- [28] P.J. Krusic, D.C. Roe, Gas-phase NMR technique for studying the thermolysis of materials: thermal decomposition of ammonium perfluorooctanoate, *Anal. Chem.* 76 (2004) 3800–3803, <https://doi.org/10.1021/ac049667k>.
- [29] T.J. Mason, J.P. Lorimer, D. Bates, Quantifying sonochemistry: casting some light on a ‘black art’, *Ultrasonics* 30 (1992) 40–42, [https://doi.org/10.1016/0041-624X\(92\)90030-P](https://doi.org/10.1016/0041-624X(92)90030-P).
- [30] R.M. Sellers, Spectrophotometric determination of hydrogen peroxide using potassium titanium(IV) oxalate, *Analyst* 105 (1980) 950–954, <https://doi.org/10.1039/AN9800500950>.
- [31] C.A. Wakeford, R. Blackburn, P.D. Lickiss, Effect of ionic strength on the acoustic generation of nitrite, nitrate and hydrogen peroxide, *Ultrason. Sonochem.* 6 (1999) 141–148, [https://doi.org/10.1016/S1350-4177\(98\)00039-X](https://doi.org/10.1016/S1350-4177(98)00039-X).
- [32] K. Johnson, R. Goody, The original Michaelis constant: translation of the 1913 Michaelis-Menten paper, *Biochemistry* 50 (2011) 8264–8269, <https://doi.org/10.1021/bi201284u>.
- [33] L. Rodriguez-Freire, R. Balachandran, R. Sierra-Alvarez, M. Keswani, Effect of sound frequency and initial concentration on the sonochemical degradation of perfluorooctane sulfonate (PFOS), *J. Hazard. Mater.* 300 (2015) 662–669, <https://doi.org/10.1016/j.jhazmat.2015.07.077>.
- [34] H. Hori, M. Murayama, N. Inoue, K. Ishida, S. Kutsuna, Efficient mineralization of hydroperfluorocarboxylic acids with persulfate in hot water, *Catal. Today* 151 (2010) 131–136, <https://doi.org/10.1016/j.cattod.2010.02.023>.
- [35] H. Hori, E. Hayakawa, H. Einaga, S. Kutsuna, K. Koike, T. Ibusuki, H. Kiatagawa, R. Arakawa, Decomposition of environmentally persistent perfluorooctanoic acid in water by photochemical approaches, *Environ. Sci. Technol.* 38 (2004) 6118–6124, <https://doi.org/10.1021/es049719n>.
- [36] M.Y. Pletnev, Chemistry of surfactants, in: V.B. Fainerman, D. Möbius, R. Miller (Eds.), *Surfactants Chem. Interfacial Prop. Appl. Vol. 13*, first ed., Elsevier, 2001, pp. 1–97, [https://doi.org/10.1016/S1383-7303\(01\)80062-4](https://doi.org/10.1016/S1383-7303(01)80062-4).
- [37] M.P. Krafft, J.G. Riess, Selected physicochemical aspects of poly- and perfluoroalkylated substances relevant to performance, environment and sustainability-Part one, *Chemosphere* 129 (2015) 4–19, <https://doi.org/10.1016/j.chemosphere.2014.08.039>.
- [38] Supeno, P. Kruus, Sonochemical formation of nitrate and nitrite in water, *Ultrason. Sonochem.* 7 (2000) 109–113, [https://doi.org/10.1016/S1350-4177\(99\)00043-7](https://doi.org/10.1016/S1350-4177(99)00043-7).
- [39] J. Rumble, *CRC Handbook of Chemistry and Physics*, 98th ed., CRC Press, Boca Raton, 2017, Doi: 10.1016/B978-0-12-408129-1.09982-4.
- [40] F. Wang, K. Shih, X. Lu, C. Liu, Mineralization behavior of fluorine in perfluorooctanesulfonate (PFOS) during thermal treatment of lime-conditioned sludge, *Environ. Sci. Technol.* 47 (2013) 2621–2627, <https://doi.org/10.1021/es305352p>.